

## Supporting information

### **A Highly Reversible Zinc Deposition for Flow Batteries Regulated by Critical Concentration Induced Nucleation**

*Shengnan Wang,<sup>†ab</sup> Ziyuan Wang,<sup>†cd</sup> Yanbin Yin,<sup>\*a</sup> Tianyu Li,<sup>a</sup> Nana Chang,<sup>ab</sup> Fengtao Fan,<sup>c</sup> Huamin Zhang,<sup>a</sup> Xianfeng Li<sup>\*a</sup>*

*<sup>a</sup> Division of Energy Storage, Dalian National Laboratory for Clean Energy, Dalian Institute of Chemical Physics, Chinese Academy of Sciences, 457 Zhongshan Road, Dalian 116023, China.*

*<sup>b</sup> University of Chinese Academy of Sciences, Beijing 100049, China.*

*<sup>c</sup> State Key Laboratory of Catalysis, Dalian National Laboratory for Clean Energy, Collaborative Innovation Center of Chemistry for Energy Materials (iChEM), Dalian Institute of Chemical Physics, Chinese Academy of Sciences, 457 Zhongshan Road, Dalian 116023, China.*

*<sup>d</sup> Collaborative Innovation Center of Chemistry for Energy Materials (iChEM), College of Chemistry and Chemical Engineering, Xiamen University, Xiamen 361005, China*

## Experimental section

*Materials:* Zinc bromide (Israel Chemicals), Potassium chloride (DAMAO Chemical Reagent Factory, Tianjin, China), Carbon felt (Liaoyang J-Carbon Materials Co., Ltd., China) and Graphite plate electrodes (Jiangsu Shenzhou carbon product Co., Ltd) were used as received. The Nafion 212 membrane was purchased from Dupont. All electrolytes were prepared with deionized water.

*Characterization:* The morphologies of Zn deposits were characterized by scanning electron microscopy (SEM, JSM-7800F). The X-ray diffraction (XRD) patterns of deposits were tested using an X-ray diffractometer (D8 ADVANCE ECO; RIGAKU, Japan). The super depth surface profile measurement microscope (VK-8550) was used to test surface fluctuation, and the magnification of sample is 400 on 15" monitor. Microhardness measurements were performed on the deposits after removing the inhomogeneous top layers using a Vickers microhardness tester (AMH43, Leco, USA) under a 5 g load and 15 s holding time. The samples used in the above characterization were all obtained after plating 30 minutes under the condition of 40 mA cm<sup>-2</sup> in different concentration Zn<sup>2+</sup> electrolytes.

*Electrochemical Measurements:* Galvanostatic deposition tests were conducted by plating metallic zinc on graphite plates with a fixed capacity of 20 mAh cm<sup>-2</sup> at a current density of 40 mA cm<sup>-2</sup>. Chronoamperometry and cyclic voltammetry (CV) tests were conducted on an electrochemical workstation (INTERFACE1000, Gamry, USA) with a three-electrode system where glassy carbon was used as working electrode, zinc plate as counter electrode and saturated calomel (SCE) as the reference electrode in the electrolytes at different concentrations. The current transient curves in chronoamperometry were obtained by applying an initial potential range from -1.16 to -1.2 V vs. SCE during 10 s, in all cases the initial potential was 0 V vs. SCE.

*In situ AFM measurements:* Highly oriented pyrolytic graphite (HOPG) was used as the working electrode, and Zn wire was used as the counter electrode and the reference electrode. Electrochemical deposition was conducted on the CHI760E workstation with a current of 10 mA cm<sup>-2</sup>. *In situ* topographical imaging (PeakForce tapping Mode) of Zn in liquid was performed using commercial SCANASYST-FLUID+ probe on Dimension ICON atomic force microscope (Bruker). The optical images were taken with Bruker's own optical microscope. The height information was analyzed by Nanoscope analysis software.

*GP//Zn Flow Cell Tests:* GP||Zn flow cells were assembled with Zn plate attached carbon felt used as

cathode, graphite plate used as anode and Nafion 212 membrane. The different concentration electrolytes were used to flow past the cells. They were operated with a charge capacity of 20 mAh cm<sup>-2</sup> at a current density of 40 mA cm<sup>-2</sup>. All the battery performance tests were conducted by CT-4008, NEWARE Battery Testing System.

*Full battery test with zinc-bromine flow battery:* The assembly method of full battery is the same as GP||Zn flow cell, except that the cathode only use carbon felt. The 2 M electrolyte was used here. The battery was operated at a constant current density of 40 mA cm<sup>-2</sup>. The battery test was conducted by CT-4008, NEWARE Battery Testing System.

*DFT calculations:* DFT calculations were performed using the Vienna ab initio simulation package (VASP)<sup>[1]</sup> with the projector-augmented wave (PAW)<sup>[2]</sup> method. All calculations were based on the same generalized gradient approximation (GGA)<sup>[3]</sup> method with Perdew-Burke-Ernzerhof (PBE)<sup>[4]</sup> functional for the exchange-correlation term. The plane wave cutoff was set to 450 eV. The Brillouin zone integration was carried out with 10×10×1 Gamma point. The convergence thresholds for energy was set as 10<sup>-5</sup> eV during ion relaxation, and the convergence thresholds for force was set as 0.05 eV Å<sup>-1</sup>.

Table S1. Surface energy corresponding to each crystal plane.

Crystal face	(002)	(100)	(101)	(102)	(103)	(110)	(004)
Surface energy (eV)	0.3099	0.6151	0.7641	0.9056	1.0814	1.4110	0.3597

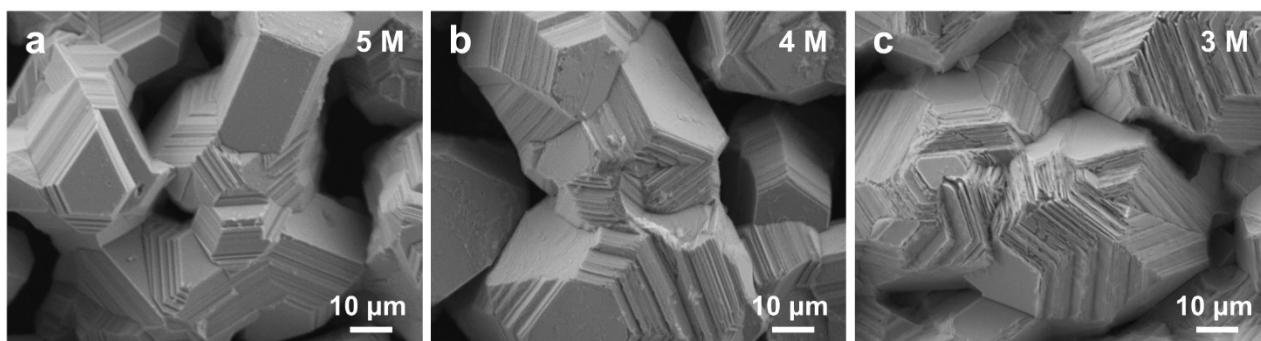


Figure S1. SEM images of Zn deposits in (a) 5, (b) 4 and (c) 3 M  $Zn^{2+}$  electrolytes after plating for 30 mins at  $40 \text{ mA cm}^{-2}$  on graphite plates.

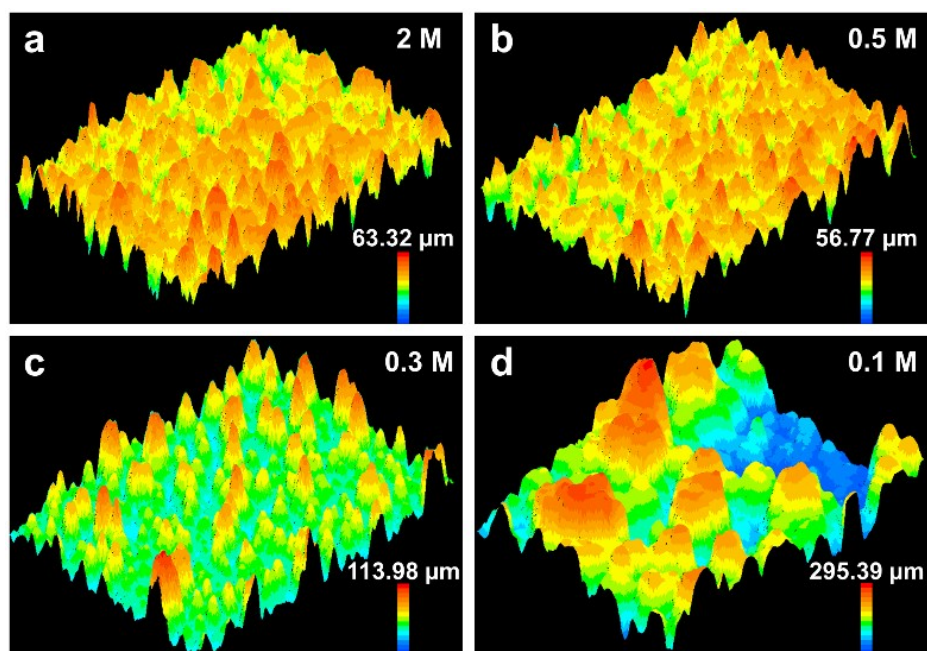


Figure S2. Surface fluctuation of different concentration Zn deposits.

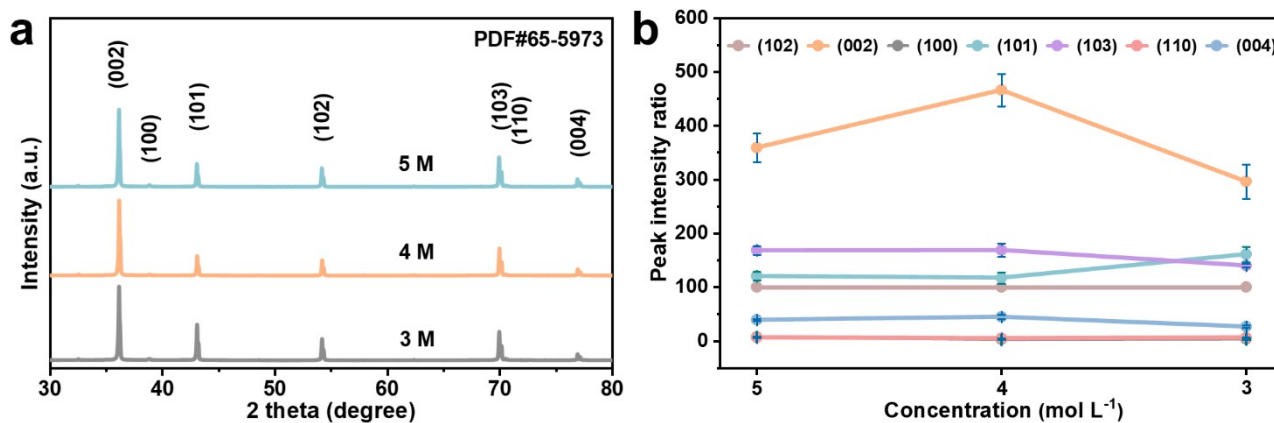


Figure S3. (a) XRD patterns of Zn after electroplating in 5, 4 and 3 M Zn<sup>2+</sup> electrolytes. (b) The average peak intensity ratio of crystal planes to (102) plane.

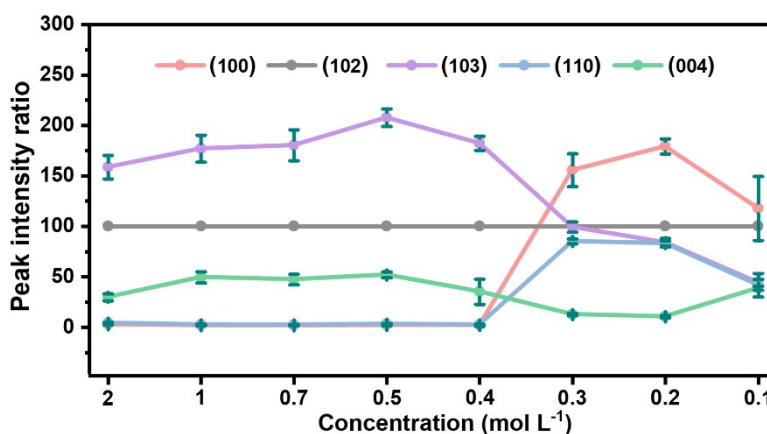


Figure S4. The average peak intensity ratio of other crystal planes to (102) plane.

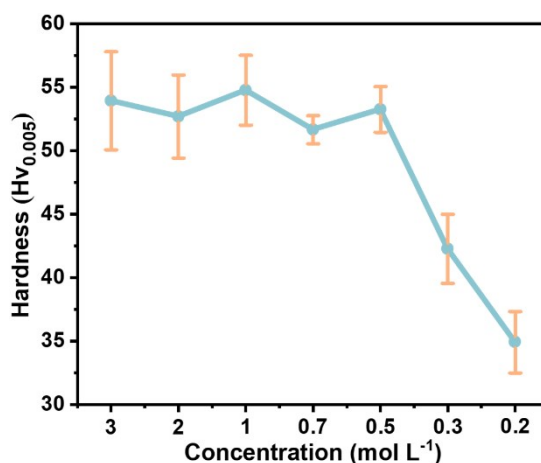


Figure S5. Microhardness of different concentration Zn deposits after plating for 30 minutes at 40 mA cm<sup>-2</sup>.

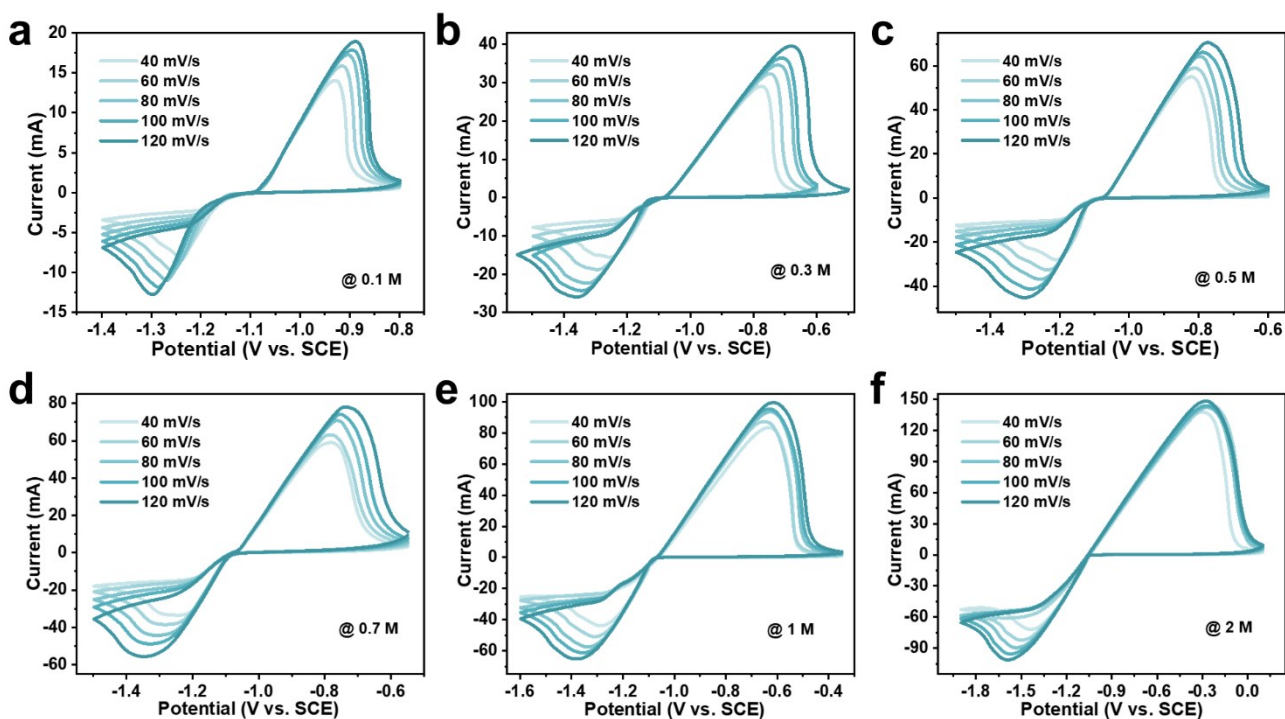


Figure S6. CV curves at a series of scan rate in different  $\text{Zn}^{2+}$  concentration electrolytes.

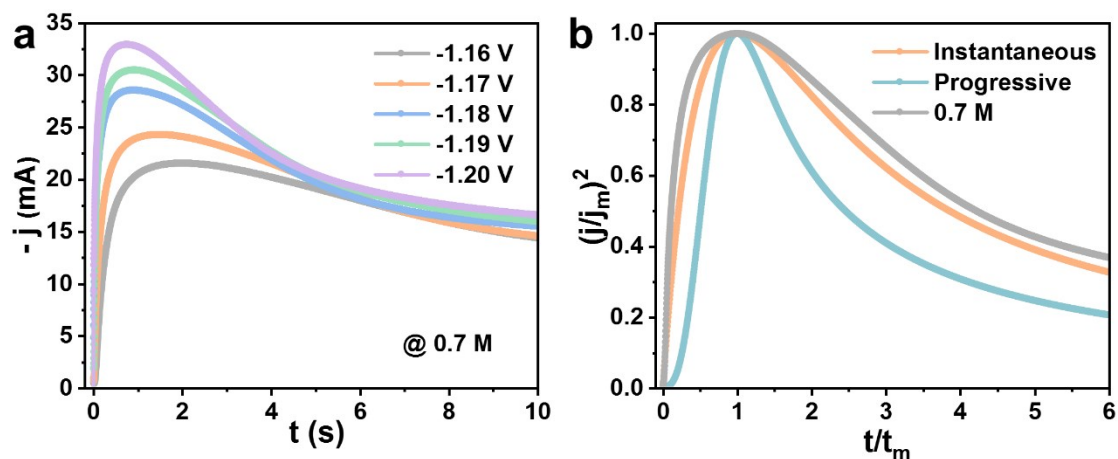


Figure S7. (a) Chronoamperograms measured at a series of potentials in 0.7 M electrolyte. (b) Comparison of the theoretical dimensionless plots for instantaneous and progressive nucleation to the experimental nucleation process in 0.7 M electrolyte.

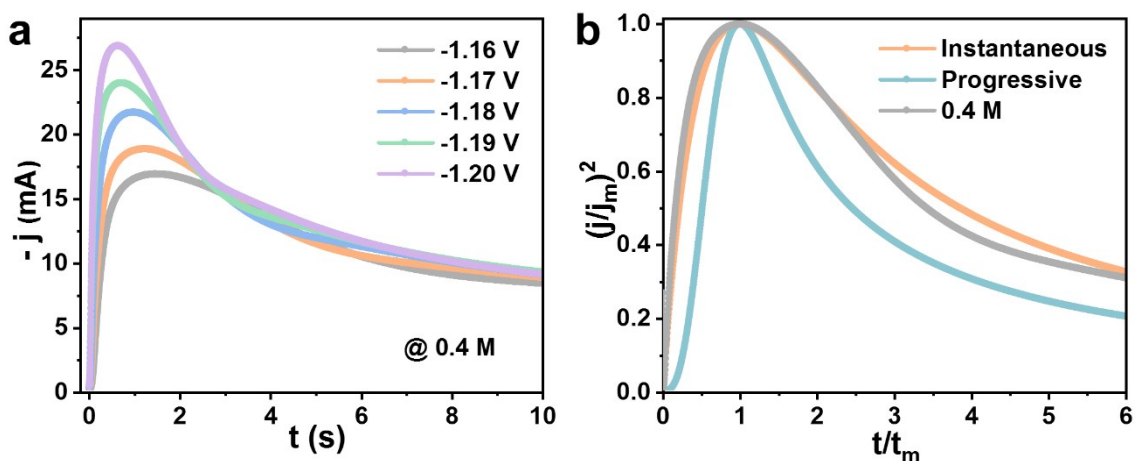


Figure S8. (a) Chronoamperograms measured at a series of potentials in 0.4 M electrolyte. (b) Comparison of the theoretical dimensionless plots for instantaneous and progressive nucleation to the experimental nucleation process in 0.4 M electrolyte.

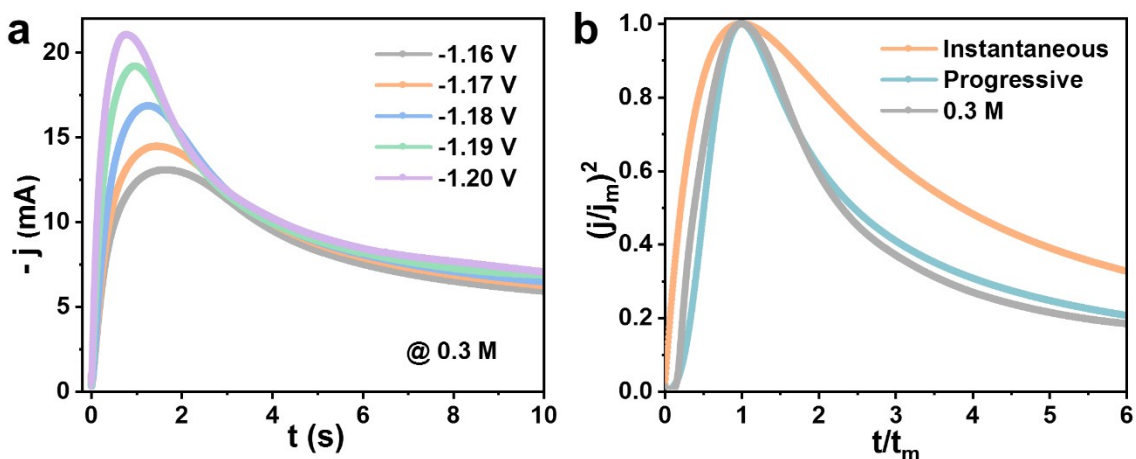


Figure S9. (a) Chronoamperograms measured at a series of potentials in 0.3 M electrolyte. (b) Comparison of the theoretical dimensionless plots for instantaneous and progressive nucleation to the experimental nucleation process in 0.3 M electrolyte.

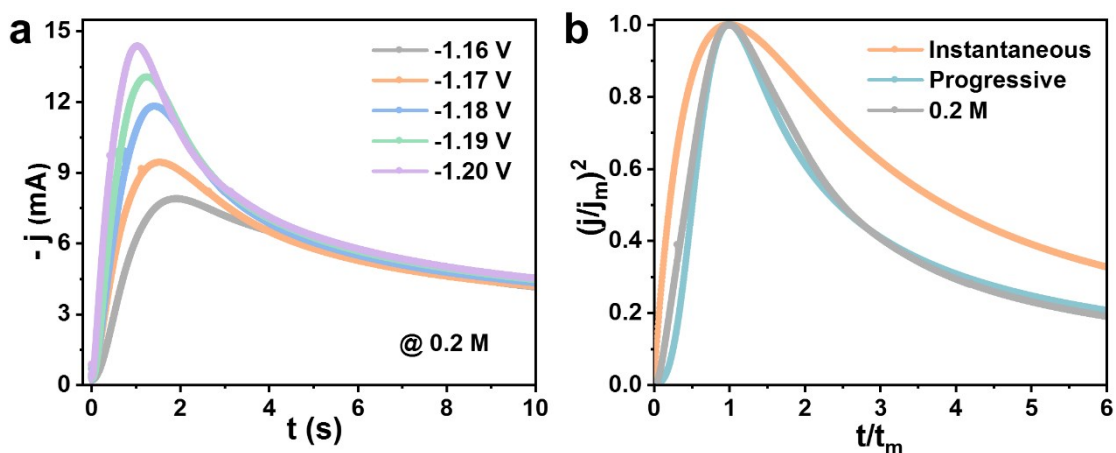


Figure S10. (a) Chronoamperograms measured at a series of potentials in 0.2 M electrolyte. (b) Comparison of the theoretical dimensionless plots for instantaneous and progressive nucleation to

the experimental nucleation process in 0.2 M electrolyte.

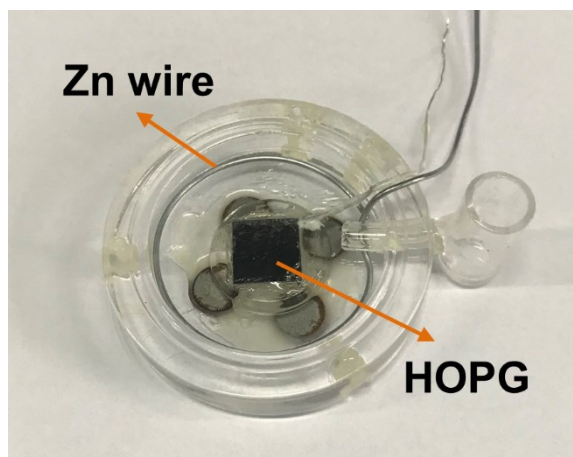


Figure S11. The digital image of sample cell using in *in situ* AFM measurement.

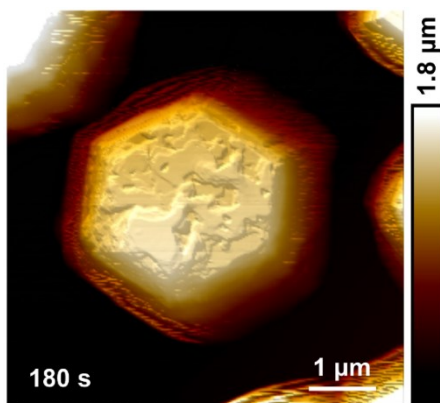


Figure S12. *In situ* AFM image of Zn electrodeposit with a current of  $10 \text{ mA cm}^{-2}$  in 0.1 M electrolyte after 180 s.

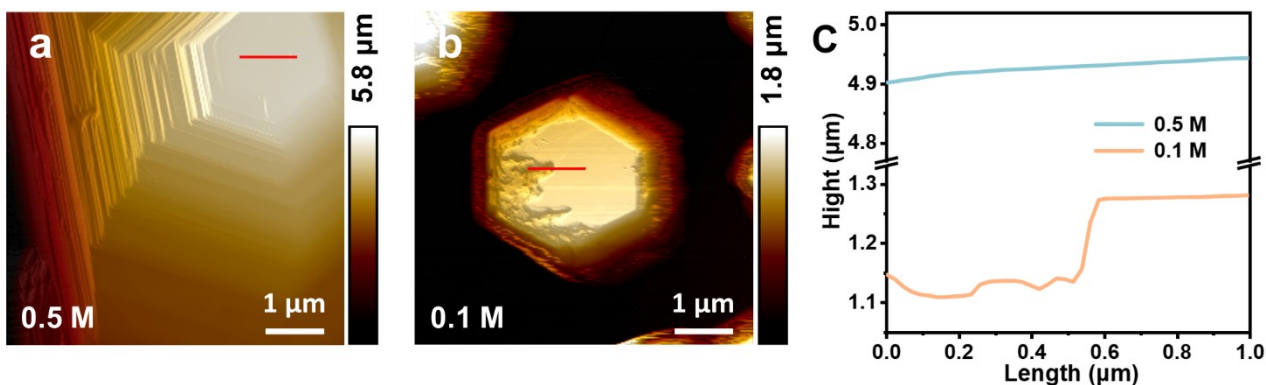


Figure S13. The corresponding height information removing the substrate at the solid lines in (a) and (b).



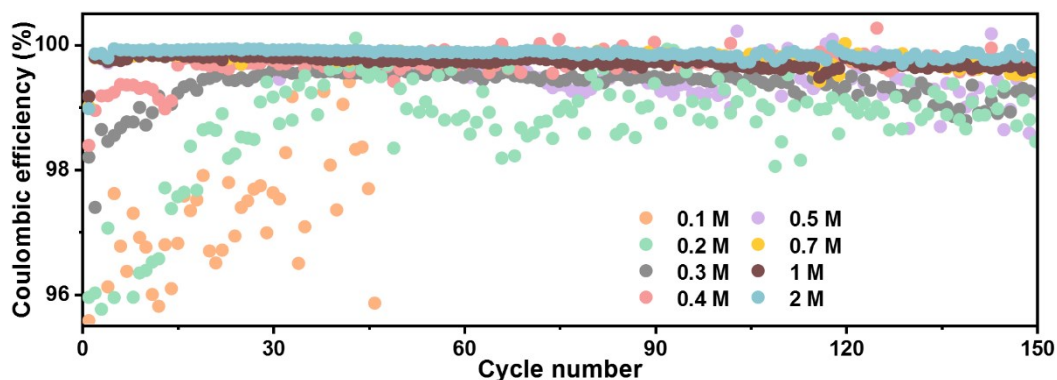


Figure S14. The long-term reversibility of GP||Zn flow cells with different  $\text{Zn}^{2+}$  concentration at a current density of  $40 \text{ mA cm}^{-2}$ .

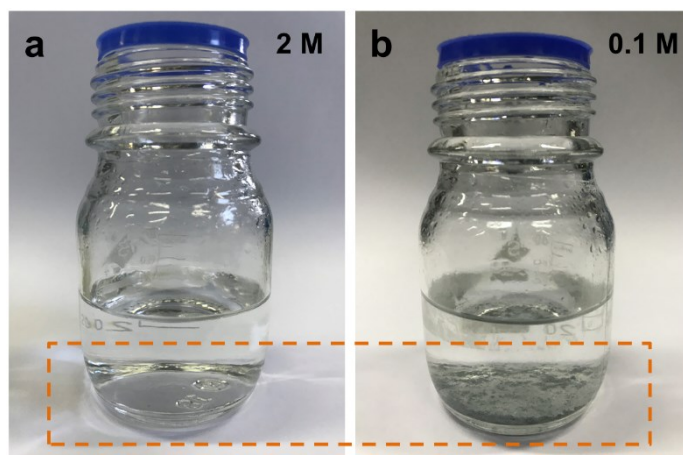


Figure S15. The fallen dead zinc in electrolyte tank of GP||Zn flow cells using 2 M and 0.1 M electrolytes at  $40 \text{ mA cm}^{-2}$  after 30 cycles.

## References

- [1] G. Kresse and J. Furthmüller, *Phys. Rev. B* 1996, **54**, 11169-11186.
- [2] P. E. Blöchl, *Phys. Rev. B* 1994, **50**, 17953-17979.
- [3] J. P. Perdew, K. Burke and M. Ernzerhof, *Phys. Rev. Lett.* 1996, **77**, 3865-3868.
- [4] J. P. Perdew, M. Ernzerhof and K. Burke, *J. Chem. Phys.* 1996, **105**, 9982-9985.